Journal Of Investment Management, Vol. 15, No. 2, (2017), pp. 65–91

www.joim.com

THE IMPACT OF DIFFERENT DEFAULT TRIGGERS ON CMBS RISK EVALUATION

Andreas D. Christopoulos[a]

This paper presents a structural generalization for pricing commercial mortgage backed securities (CMBS) and their derivatives, CMBX. I compare results for the structural generalization with a reduced-form approach using identical data sets and analyses. My comparisons are made at both the loan and bond levels and cover the period November 2007 through June 2015 using $389 billion of loans serving as the underlying collateral for CMBX Series 1 through 8. The sole difference between the two modelling approaches is found in the set of conditions and methods for simulating the default event which together comprise the 'default trigger' that differ for each model. I statistically validate the default estimations and then construct an automated long/short trading strategy using the risk measure Theta to compare the impact of default estimates on investment and risk management decision making. The findings indicate the reduced form provides greater precision than the structural generalization in estimating default events and in assessing trading opportunities.

1 Introduction

This paper presents a generalized structural model for pricing CMBS and then compares valuation and risk assessment results with a reduced-form model using an identical data set which is filtered identically. The ~$1T CMBS market is an important source of financing, accounting for about 20% of all new commercial real estate borrowing in the U.S. As the CMBS market does not utilize derivatives pricing technology as discussed in Christopoulos and Jarrow *et al.* (2014) and given persistent volatility in the sector from the time of the crisis up to the present day as described in Fung (2016), Penner (2016), and Chandan (2012), among others, an investigation into the evaluation of CMBS risk remains an important topic for academics, practitioners, and regulators.

Evaluation of the pricing of risks of default as found in the literature in CMBS in Titman and Torous (1989) and more recently in the credit

[a]The University of Texas at Austin, McCombs School of Business, Austin, TX 78712-1276, Phone: 512-471-6506, E-mail: andreas.christopoulos@mccombs.utexas.edu

spread literature as found in Chen *et al.* (2007), Driessen (2005), and Gilchrist and Zakrajšek (2012), among others, has important implications for estimations of liquidity premia and risk policy as found in Bao *et al.* (2016). This paper provides important insights related to default risk for CMBS across two well-regarded model approaches.

Commercial real estate loans (CRELs) in trusts exhibit considerable heterogeneity with respect to the amount and timing of cashflows. These differences may materially influence the risks facing investors which may influence their perceptions of risk which are then impounded into market pricing. Because of the importance of cashflows to assessments by investors, this study makes a substantial effort to preserve the realism of loan and bond characteristics by implementing the following important developments which are rare in the literature: (i) Accurate loan level principal and interest cashflows; (ii) accurate bond tranche cashflow allocations from the loans; (iii) categorization of a broad set of real estate property types; (iv) flexibility to allow for both term and balloon defaults; and (v) a robust multi-factor economy consisting of interest rates, property values and REITs. With these non-trivial developments, which are rare in the literature, I am able to robustly evaluate the loans underlying 1/3 of the CMBS universe and I am also able to evaluate the risk-neutral pricing of CREL risks at the bond level using two approaches: the structural hybrid[1] and the reduced form.[2]

I construct an arbitrage free pricing model to price CMBS bonds and then construct trading strategies to exploit market mispricings. I test the performance of my trading strategies over the time period November 2007 to June 2015. Fair value prices for CMBX tranches are determined under the assumption that the loan collateral securing the CMBS tranches serves as the cashflow generating collateral for the CMBX tranches. In this way, CMBX in this study are essentially very large CMBS secured directly by loan cashflows and not by bond cashflows (secured by loan cashflows). The loan to bond cashflow tranching algorithm is described in Equation (18).

Since CMBX are derivatives of CMBS, the loan cashflows securing said CMBS nevertheless represent the fundamental source of default risk for CMBX instruments. As such, the pricing of such CMBX instruments should accurately reflect the risks at the loan level and they do not. This finding is consistent with those of Stanton and Wallace (2011) who find that the pricing of Markit's other product, ABX.HE, collateralized by subprime mortgage cashflows, is also not congruent with the loan collateral default risks.

Additionally, as CMBX trade far more frequently than cash CMBS and as long/short strategies for both hedging and construction of synthetic exposure are widely implemented with these instruments and cannot generally be implemented with cash CMBS, the findings of this paper using CMBX pricing in the trade strategies are appropriate. CMBX pricing which informs the measure Theta, seems to capture the phenomenon of mispricing of loan level default risk at the CMBX bond level and suggests, further, a more broad based criticism of imprecise risk evaluation within the CMBS sector overall. Figure 1 shows cumulative returns for each of the structural model, the reduced-form model based upon trading strategies and compares them with the market portfolio and the long-only CMBS portfolio.[3] We see the cumulative return of 17% for the structural model underperforms the reduced-form portfolio (71%) and the market portfolio (39%) and only outperforms the CMBS long-only portfolio (−18%) over the sample period. These positive trade strategy findings are supported statistically in the Receiver Operating Characteristic Area

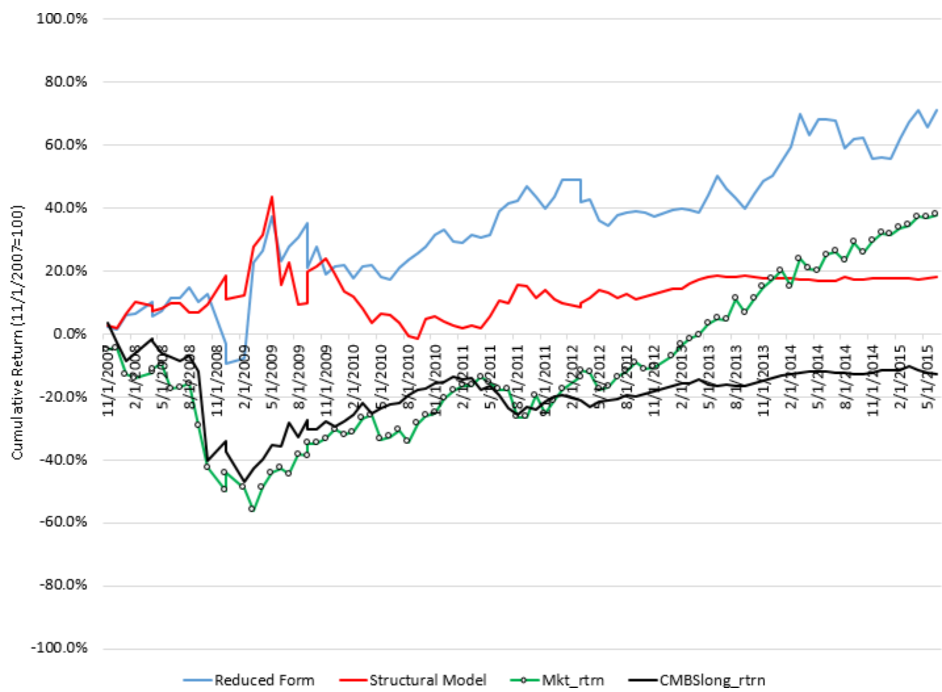

This figure shows the cumulative returns generated by the automated trading strategy for each of the structural and reduced form models. It contrasts these model driven returns with the market portfolio and the long-only CMBS sector portfolio.

Figure 1 Cumulative portfolio returns.

Under the Curve (ROC AUC) and Brier score analyses which are used for validation in the credit risk literature.

The results in this paper provide empirical support for the theoretical debate discussed in Jarrow and Protter (2004) that posits the locus of the distinction between the structural and reduced-form approach to be found in the differing information sets that may be absorbed by each model. My study suggests that the default mechanism in the structural generalization was relatively worse than the reduced form in the task of evaluation of CMBS risk in the sample period. This echoes the findings of Arora *et al.*, (2005) and others who also find relatively worse risk navigation ability in the structural approach compared with the reduced form.

The recent related CMBS literature can be split into four categories: (i) work on commercial real estate loans related to lender incentives, securitization, and the origination process (see Titman and Tsyplakov, 2010, Ghent and Valkanov, 2013; Buschbom *et al.*, 2015), (ii) work on credit risk ratings and the misclassification of loan and bond risk (see Crouhy *et al.*, 2008; Stanton and Wallace, 2012; Riddiough and Zhu, 2016), (iii) analyses of loan and bond credit spread risk premia (see Titman *et al.*, 2005, and Ambrose *et al.*, 2014), and (iv) studies investigating commercial real estate loan collateral, derivative pricing, and CMBS market efficiency (see Christopoulos *et al.*, 2008; Kau *et al.*, 2009; Hollifield *et al.*, 2016; Driessen and Van Hemert, 2012). My paper falls into this last category.

The remainder of this paper is organized as follows. I discuss the data in Section 2 at the loan, bond and economy levels. I introduce the two models in Section 3 and break out discussions of the default triggers. In Section 4 the loan cashflow and bond allocation algorithms are presented, while in Section 5 I describe the valuation of CMBS. I discuss in Section 6 the statistical validation of the model, corresponding trading strategy and its results and the comparative portfolio risk assessment is discussed. I conclude in Section 7.

2 The data

Throughout this paper, the analysis of loans and bond pricing and risk values is based upon loan and bond cashflows which have monthly payment frequencies. I have 25,019 loans in my sample from the Intex database with static origination information as well as updated monthly payment status information over the period November 2007 through June 2015. The fundamental object of risk in this study is the CRELs that represent the underlying collateral for the 200 CMBS bonds within the CMBX Series 1–8. The total principal balance represents approximately 1/3 of the entire CMBS universe outstanding. Figure 2 gives a summary of the CMBX loans and tranches included in my study.

The building block of CMBS and CMBX is the mortgage secured by the income-producing property. Commercial mortgages have a variety of cashflow timing and maturity profiles that have evolved over time to provide the borrower with important flexibility in both the purchasing of properties and refinancing of existing debt. These features which vary considerably amongst loans include: different balloon dates, different dates of expiration among loans within a trust, different amortization schedules including but not limited to level pay, balloon, interest only balloon, and combinations therein. By modelling the promised (and *actual*) principal and interest cashflows for all loans in my sample I reflect their correct timing and payment idiosyncrasies and custom restrictions.

Additionally, I have daily mark-to-market prices released by Markit for the 57 priced CMBX tranches which I use for trade strategy pricing comparisons. All the licensed market-makers in CMBX provide daily closing prices to Markit. Markit then aggregates these prices and distributes them to its customers at the end of each trading day (4:15 PM EST). I only determine fair prices for the CMBX tranches (not underlying reference tranches) under the assumption that the loan collateral securing the CMBS tranches serves as the cashflow generating collateral for the CMBX tranches. Each CMBX index has 6–7 tranches. I model the top 6 tranches for

	CMBX Series								
Loan Property Type	Series 1	Series 2	Series 3	Series 4	Series 5	Series 6	Series 7	Series 8	Total
Industrial	*547*	*529*	*613*	*581*	*447*	*200*	*189*	*249*	*3355*
Lodging	*256*	*401*	*437*	*446*	*283*	*238*	*225*	*230*	*2516*
Multifamily	*701*	*387*	*378*	*347*	*162*	*251*	*482*	*496*	*3204*
Office	*834*	*809*	*933*	*974*	*634*	*269*	*192*	*290*	*4935*
Other	*107*	*158*	*228*	*248*	*205*	*85*	*88*	*99*	*1218*
Retail	*1559*	*1606*	*1833*	*1822*	*1414*	*544*	*491*	*522*	*9791*
Total # Loans	4004	3890	4422	4418	3145	1587	1667	1886	25019
Total Loan Balance ($bln)	$57.80	$55.10	$71.90	$72.20	$49.90	$29.90	$27.50	$25.10	$389.40

This table provides the number of loans in the aggregate and by property type for each of the CMBX Series 1–8. It also provides the original loan balances for each Series.

Figure 2 Summary counts of underlying loans for CMBX Series 1 thru 8.

each CMBX: $\ddot{k} \in \{AAA, AJ/AS, AA, A, BBB, BBB-\}$ which are the most actively traded.[4] The first four CMBX series (Series $1, \ldots, 4$) were issued prior to 11/2007; Series 5 was issued in 5/2008; Series 6–8 were issued annually in the month of January between 2013 and 2015. Therefore, the total number of bonds available to construct my trading strategies is $6 \cdot J$ where

$$\ddot{J} = \begin{cases} 4, & time: \ 10/2007 - 5/2008 \\ 5, & time: \ 5/2008 - 12/2012 \\ 6, & time: \ 1/2013 - 12/2013 \\ 7, & time: \ 1/2014 - 12/2014 \\ 8, & time: \ 1/2015 - 6/2015. \end{cases} \tag{1}$$

Since the object of inquiry here is ultimately the derivative of bonds which are at the most granular level still collateralized by loan cashflows, and since my simulation is at the loan level, the aggregation of the simulated cashflows up to the bond and trust levels can be compared with the market observable prices in the secondary market for bond and CMBX[5] derivatives.

For the simulated economy I have property $\times$ regional property indices from the National Council of Real Estate Investment Fiduciaries (NCREIF). Property value indices were provided by NCREIF. These indices are obtained quarterly and correspond to 8 regions: east north central, mid-east, mountain, north-east, pacific, south-east, south-west, and west-north for 6 property types. This gives a total of 48 different (property $\times$ regional) indices which are simulated as described below.

I also have interest rate data provided through the Federal Reserve Board and property-specific REITs listed in Figure 3 aggregated by Yahoo! Finance from primary pricing data provided by the stock exchanges associated with such REITs (NYSE, NASDAQ, and AMEX) as the primary source. REIT debt levels and 90-day volatilities

Ticker	REIT Name	Property Type
AVB	AVALONBAY COMMUNITIES	MF
BKD	BROOKDALE SENIOR LIVING	OT
BMR	BIOMED REALTY TRUST	IN
BRE	BRE PROPERTIES	MF
BXP	BOSTON PROPERTIES	OF
CLI	MACK-CALI REALTY	OF
DDR	DDR CORP	RT
DRE	DUKE REALTY	IN
ELS	EQUITY LIFESTYLE PROPERTIES	MF
EQR	EQUITY RESIDENTIAL	MF
ESC	EMERITUS CORP	OT
FCH	FELCOR LODGING TRUST	LO
FR	FIRST INDL REALTY TRUST	IN
GRT	GLIMCHER REALTY	RT
HCN	HEALTH CARE REIT	OT
HIW	HIGHWOODS PROPERTIES	OF
HOT	STARWOOD HOTELS & RESORTS	LO
HST	HOST HOTELS & RESORTS	LO
KIM	KIMCO REALTY	RT
LHO	LASALLE HOTEL	LO
LRY	LIBERTY PROPERTY	OF
NNN	NATIONAL RETAIL	OT
PLD	PROLOGIS	IN
PSB	PS BUSINESS PARKS	OT
REG	REGENCY CENTERS	RT
SPG	SIMON PROPERTY GROUP	RT
SSS	SOVRAN SELF STORAGE	IN
TCO	TAUBMAN CENTERS	RT
UDR	UNITED DOMINION	MF
VNO	VORNADO REALTY TRUST	OF
WPC	WP CAREY	OT

This table provides the list of the REITs which are aggregated into property type indices and then simulated.

Figure 3 List of REITs underlying property type diffusions.

for REITs and the S&P 500 were provided by Wharton Research Data Services (WRDS).

The loan, bond, deal, NCREIF indices, and Markit CMBX pricing were generously donated to me for my research by an anonymous institutional investor with ~\$0.50 trillion assets under management.

3 The models

The purpose of this section is to describe the components of the modelled economy and the distinct default processes. In Step 1 I determine the calibrated parameters while in Step 2 I discuss the term structure of interest model. In Step 3 I simulate the economy informed by the parameters while in Step 4 I consider two ways (the structural and the reduced form) to link the loan-level characteristics to the simulated economy to trigger default events for loans in the sample thereby generating the random cashflows that reflect the loan-level credit risks underlying CMBX.

3.1 Step 1: *Calibrated REIT property values*

In this step the parameters are the outputs of a numerically solved non-linear system of six equations which calibrate to daily S&P option volatility, REIT pricing covariances and other observable market metrics relevant to simulation and CREL valuation. The parameters determined in the calibration by solving the system consisting of Equations (2,3,4,5, and 6) include sector-level property volatilities ($\gamma_1, \ldots, \gamma_6$), betas ($\beta_1, \ldots, \beta_6$) for the S&P 500, property type sector correlations ($\rho_{12}, \rho_{13}, \ldots, \rho_{45}, \rho_{56}$), idiosyncratic property volatilities ($\sigma_1, \ldots, \sigma_6$), stock market volatility $\sigma_{s\&p}$,and the latent property value for each of the sector-level REIT indices ($\bar{V}_{1t}, \ldots, \bar{V}_{6t}$).[6] This approach is an extension of the standard approach used to extract asset values and asset volatilities from equity prices and equity volatilities.

The variables E_j and E_k are the daily average equity market capitalizations within REIT property-type sector $j, k = 1, \ldots, 6$ across the 31 property-type sector-specific REITs selected.[7] Specifically an REIT index is computed as a weighted sum for each property type based on market capitalization. There are six such indices (1 for each property type) and within each property type there are a set of REITS. There are five REITs contained Multifamily ($j = 1$), five REITs contained in Office ($j = 2$), six REITs contained in Retail ($j = 3$), five REITs contained in Industrial ($j = 4$), four REITs contained in Hotels ($j = 5$), and six REITs contained in Other ($j = 6$) which are diversified across more than one property type. The variance of the stock index $\sigma^2_{s\&p}$ is calculated from the pricing of 3-month (90-day) ATM S&P 500 options. The debt variable D_j is the indexed property-specific REIT debt principal value outstanding calculated by taking the daily average of the sum of (long term debt + current liabilities) within property-type sector $j, k = 1, \ldots, 6$ across the 31 property-type sector-specific REITs. The maturity date for REIT debt is assumed to be 5years.[8] The risk-free rate r is determined from 5year and 10year swap rates (for each calibration date) as the corresponding linearly interpolated rate. I assume a dividend rate $q = 0\%$ based on the assumption of low income derived from the properties compared with capital appreciation and because dividends do not appear in the reduced-form model which I will ultimately compare with the structural model.

Following Driessen and Van Hemert (2012) the parameters are calibrated within the restrictions of the simultaneous equations as follows:

First,

$$E_j = BSM(\beta_j^2\sigma^2_{s\&p} + \gamma_j^2, \bar{V}_j, \bar{D}_j, \bar{T}_j), \quad j = 1, \ldots, 6 \qquad (2)$$

defines the total equity value of the REIT corresponding to each sector j where $BSM(., ., .,)$ represents the Black–Scholes–Merton call price formula as a function of volatility, price, strike and maturity, respectively. *Second*, the variance of the REIT equity returns is defined as

$$Var\left(\frac{dE_j}{E_j}\right) = \left(\frac{\bar{V}_j \partial E_j}{E_j \partial \bar{V}_j}\right) Var\left(\frac{d\bar{V}_j}{\bar{V}_j}\right) = \left(\frac{\bar{V}_j \partial E_j}{E_j \partial \bar{V}_j}\right)^2 \left(\beta_j^2\sigma^2_{s\&p} + \gamma_j^2\right) dt, \quad j = 1, \ldots, 6 \qquad (3)$$

Third, we have the covariance of REIT equity with the stock market index,

$$Cov\left(\frac{dE_j}{E_j}, \frac{dM}{M}\right) = \left(\frac{\bar{V}_j \partial E_j}{E_j \partial \bar{V}_j}\right) \beta_j^2 \sigma_{s\&p}^2 dt, \quad j = 1, \ldots, 6 \tag{4}$$

Fourth, we have the covariance of the REIT returns across different sectors,

$$\begin{aligned} Cov\left(\frac{dE_j}{E_j}, \frac{dE_k}{E_k}\right) &= \left(\frac{\bar{V}_j \partial E_j}{E_j \partial \bar{V}_j}\right)\left(\frac{\bar{V}_k \partial E_k}{E_k \partial \bar{V}_k}\right) \beta_j \beta_k \sigma_{s\&p}^2 dt \\ &+ \left(\frac{\bar{V}_j \partial E_j}{E_j \partial \bar{V}_j}\right)\left(\frac{\bar{V}_k \partial E_k}{E_k \partial \bar{V}_k}\right) \rho_{j,k} \gamma_j \gamma_k dt, \\ & j = 1, \ldots, 6 \end{aligned} \tag{5}$$

And finally, *Fifth*, we have the variance of the stock index return equal to $\sigma_{s\&p}^2 dt$ as:

$$Var\left(\frac{dS}{S}\right) = \sigma_{s\&p}^2 dt \tag{6}$$

For each of the previous equations the values on the left-hand side (LHS) of the equation are observed historical data. These values are then equated to the right-hand side (RHS) such that the outputs are the *calibrated parameters* that satisfy the requirements of the system of equations. This *calibration procedure* is conducted on each simulation date in the sample period.

The equity volatility term instead of being observed as in Merton (1974) is now a composite term of the known volatility on the S&P 500 index $\sigma_{s\&p}$, and REIT property-type parameters β_j and γ_j which are solved for numerically, such that:

$$d_{1,j} = \frac{ln\left(\frac{V_j}{D_j}\right) + \left(r + \frac{\sigma_j^2}{2}\right) T}{\sigma_j \sqrt{T}} \quad \text{and}$$

$$d_{2,j} = d_{1,j} - \sigma_j \sqrt{T} \tag{7}$$

where the Black–Scholes–Merton condition is given by:

$$E_j = V_j \mathrm{N}(d_{1,j}) - D_j e^{-rT} \mathrm{N}(d_{2,j}) \tag{8}$$

and the condition satisfying Ito's Lemma in parametrized form is then given by:

$$(\beta_j \sigma_{s\&p} + \gamma_j) E_j = V_j \sigma_j \mathrm{N}(d_{1,j}) \tag{9}$$

I numerically solve the non-linear system of equations simultaneously using the standard optimization

$$\min \| f(x) \|_2^2 = \min (f_1(x)^2 + f_2(x)^2 + \cdots f_{40}(x)^2) \tag{10}$$

which yields outputs for the 40 calibrated parameters to observed option prices and other data for the sample period on daily basis.

The charts in Figure 4 show the numerically determined calibrated outputs from the solved system above. The system is solved for 1,892 consecutive trading days. Figure 4, Panel A captures the numerically determined volatility parameter, σ_j, while latent property values, V_j, are captured in Figure 4, Panel B. There is substantial variability in the results with respect to time which makes intuitive sense. Prior to the crisis as property values were increasing, volatility in the marketplace was muted. As the crisis period ensues, volatility increased with concomitant declines in property values. As the crisis wanes, volatility decreases and property values, once again, increased. This intuition is borne out in the plots which show property volatility increases/decreases (Figure 4, Panel A) within the crisis/recovery while latent property values captured in the REITs decline/increase (Figure 4, Panel B) within the crisis/recovery, as expected.

Additionally, captured correlations amongst the REITs (Figure 4, Panel C) are all between −1

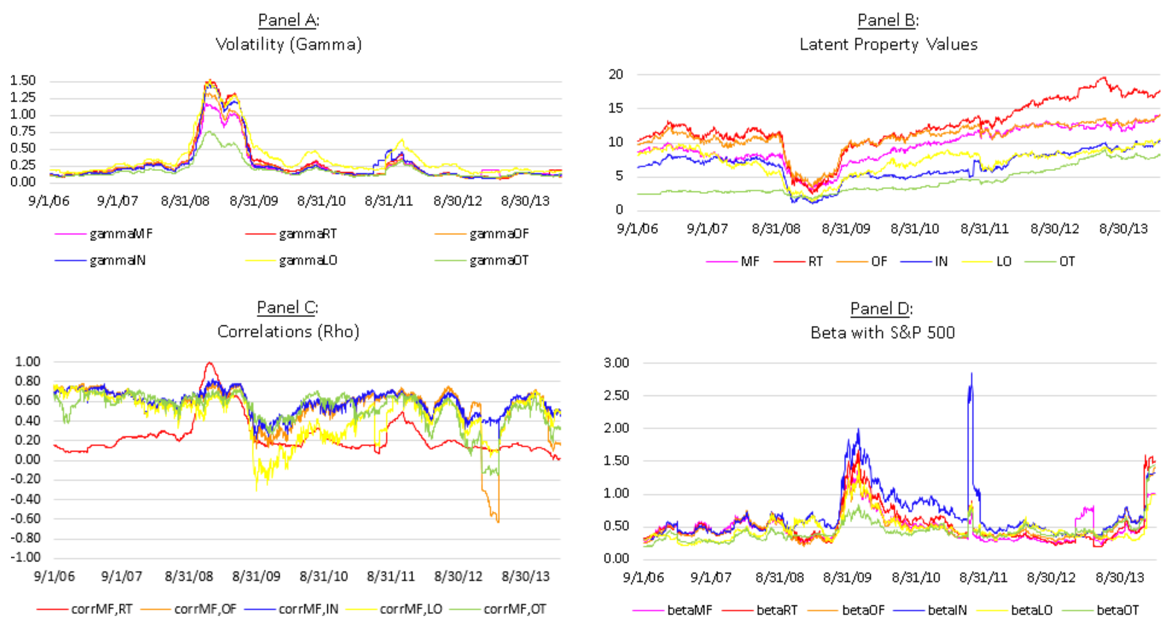

The panels in this figure show the output values determined from the historical calibration for each of the property types. Panel A shows the calibrated volatility while Panel B shows the latent property values.

Panel C shows pairwise with the multifamily (MF) property type while Panel D shows the implied beta with with stock market index.

Figure 4 Calibration parameters.

and 1 with Hotels and Office exhibiting the greatest fluctuations. This is reflected further in the betas of Hotels and Office (Figure 4, Panel D) which indicate greatest amplification of value with the S&P 500 which makes sense as Hotels are generally considered to be among the most capricious of property types, most directly reflecting changes in consumer sentiment and business spending. As both property type volatility and latent property values for REITs are used to capture the simulated default event for the structural model in Equations (13) and (15) the fact that these empirically determined results make intuitive sense provides support for the implementation of the accuracy of my structural generalization in keeping previous studies.[9]

3.2 *Step 2: The term structure of interest rates*

In this step I discuss the term structure of interest rates model. Interest rate risk is modelled using a multi-factor Heath, Jarrow, and Morton ('HJM', 1992) model. In this section, I specify the evolution of the term structure using forward rates under the martingale measure.

Let $f(t,T) = -\frac{\partial \log p(t,T)}{\partial T}$ be the instantaneous (continuously compounded) forward rate at time t for the future date T. I use a K- factor model HJM model.

$$df(t,T) = \alpha(t,T)dt + \sum_{j=1}^{K} \sigma_j(t,T)dW_j(t) \quad (11)$$

where K is a positive integer, $\alpha(t,T) = \sum_{j=1}^{K} \sigma_j(t,T) \int_t^T \sigma_j(t,u)du$, $\sigma_j(t,T) \equiv \min[\sigma_{rj}(T) f(t,T), M]$ for M a large positive constant, $\sigma_{rj}(T)$ are deterministic functions of T for $j = 1, \ldots, K$, and $W_j(t)$ for $j = 1, \ldots, K$ are uncorrelated Brownian Motions initialized at zero. Under this evolution, forward rates are "almost" lognormally distributed.

The spot rate process, used for valuation, can be deduced from the forward rate evolution. Noting that $r_t \equiv f(t,t)$, it can be shown that

$$dr_t = [\partial f(t,t)/\partial T]dt + \sum_{j=1}^{K} \min[\sigma_{rj}(T)r_t, M]dW_j(t) \qquad (12)$$

To estimate the forward rate process given in Equation (11) I employ a principal component analysis as discussed in Jarrow (2002). Given is a time series of discretized forward rate curves $\{f(t,T_1), f(t,T_2), \ldots, f(t,T_{N_r})\}_{t=1}^{m}$, where N_r is the number of discrete forward rates observed, the interval between sequential time observations is Δ and m is the number of observations. Then, percentage changes are computed

$$\left\{\frac{f(t+\Delta,T_1)-f(t,T_1)}{f(t,T_1)}, \ldots, \frac{f(t+\Delta,T_N)-f(t,T_{N_r})}{f(t,T_{N_r})}\right\}_{t=1}^{m}.$$

From the percentage changes, the $N_r \times N_r$ covariance matrix (from the different maturity forward rates) is computed, and its eigenvalue/eigenvector decomposition calculated. The normalized eigenvectors give the discretized volatility vectors$\{\sigma_{rj}(T_1)\sqrt{\Delta}, \ldots, \sigma_{rj}(T_{N_r})\sqrt{\Delta}\}$ for $j = 1, \ldots, N_r$. The term structure data was obtained from the Federal Reserve Board.[10] It consists of daily constant maturity yields from 1 month up to 30 years. The data set starts on June 1, 2007 and goes to June 10, 2015. I convert these constant maturity yields into a term structure of (smoothed) continuously compounded forward rates with maturities 1 month, 3 month, 6 month, 1, 2, 3, 5, 7, 10, 20, and 30 years. The estimates for the forward rate volatility coefficients and percentage variance determined from the principal component analysis are presented in Figure 5 based on monthly observation intervals ($\Delta = 1/12$) of factor volatilities $\sigma_j(T)$ for $j = 1, \ldots, 11$ and $T = 1$ months, ..., 30 years. Daily observation intervals were not used because daily variations in rates are partly caused by the smoothing procedure. Monthly observation intervals reduce the importance of this smoothing noise in the

maturities\Factors	1	2	3	4	5	6	7	8	9	10	11
1mo	0.6270	0.3660	0.2070	0.6160	0.1220	-0.1680	0.0000	0.0000	0.0000	0.0000	0.0000
3mo	0.4730	0.1900	0.2140	-0.4030	-0.4110	0.5760	-0.1620	0.0000	0.0000	0.0000	0.0000
6mo	0.3330	0.0000	0.0000	-0.5920	0.0000	-0.5050	0.4630	0.2070	-0.1300	0.0000	0.0000
1yr	0.2750	0.0000	-0.1950	-0.2570	0.3600	-0.2700	-0.6590	-0.4070	0.1300	0.0000	0.0000
2yr	0.2530	-0.1860	-0.5150	0.0000	0.3750	0.3530	0.0000	0.5340	-0.2700	0.0000	0.0000
3yr	0.2340	-0.2690	-0.4420	0.0000	0.0000	0.1500	0.4480	-0.3700	0.4860	-0.2350	-0.1440
5yr	0.1890	-0.3670	-0.1710	0.1250	-0.3880	0.0000	0.0000	-0.3160	-0.3800	0.4940	0.3720
7yr	0.1480	-0.4050	0.0000	0.1210	-0.3780	-0.2650	-0.2280	0.1420	-0.2710	-0.4820	-0.4550
10yr	0.1100	-0.4020	0.2080	0.0000	0.0000	-0.1590	-0.1840	0.4300	0.5920	0.0000	0.4190
20yr	0.0000	-0.3650	0.3920	0.0000	0.2420	0.1410	0.0000	0.0000	0.0000	0.5330	-0.5750
30yr	0.0000	-0.3570	0.4290	0.0000	0.4230	0.2060	0.1330	-0.2520	-0.2800	-0.4170	0.3570
Standard deviation	0.5882	0.2643	0.1120	0.0820	0.0459	0.0313	0.0214	0.0173	0.0126	0.0105	0.0102
% of Variance	0.7875	0.1590	0.0285	0.0153	0.0048	0.0022	0.0010	0.0007	0.0004	0.0003	0.0002
Cumulative	0.7875	0.9466	0.9751	0.9904	0.9952	0.9974	0.9985	0.9991	0.9995	0.9998	1.0000

The estimates in this table correspond to the factor volatilities $\sigma_j(T)$ for $j = 1, \ldots, 11$ and $T = 1$ month, …, 30 years obtained from a principal components analysis using monthly percentage changes in forward rates. The proportion of variance is the percentage of the variance explained by each factor. The estimation is over the time period September 2007 to June 2015.

Figure 5 Forward rate volatility.

estimated coefficients. The percentage variance represents the variance explained by each factor. The estimation is over the time period November 2007 to June 2015.

3.3 Step 3: *The correlated economy*

In this step I discuss the simulation using multivariate correlated Brownian Motions.

Using the latent property values determined in Step 1, I then apply the multivariate Brownian Motion process that generates simulated returns on REITs

$$\frac{d\bar{V}_\iota}{\bar{V}_\iota} = (r - q)dt + \sigma_\iota dW_\iota \tag{13}$$

where r denotes the risk-free rate, q the dividend rate,[11] and dW_ι the specific Brownian Motion that interact with their corresponding observed volatility term σ_ι. All ι diffusions are correlated with one another so,

$$Corr(dW_\iota, dW_\kappa) = \rho_{\iota,\kappa} dt \quad \iota, \kappa = 1, \ldots, 72 \tag{14}$$

The six property-specific REIT diffusions are simply a subset of the 72 total factors that make up the economy. These 72 factors are: 11 Forward interest rates; 48 property × regional NCREIF indices; six property-specific NCREIF indices; and six property-specific REIT indices; and one national REIT index.

The subset of six property-specific REIT indices is required by the structural model default trigger. The casting of those six REIT indices within a richer economy of 72 factors is motivated by the statistical significance for the 72 factors with events of CREL defaults.[12] This allows for simulation of pathwise defaults in both model choices. Since I correctly determine the variance-covariance matrix I am permitted to compute the Cholesky decomposition required for correlated diffusions in the simulations.[13]

3.4 Step 4: *Two different default mechanisms*

Up to this point the data inputs, treatment of the loans, and simulation of the economy for both models are identical. Both are credit-only models which abstract from prepayment and liquidity risk. Both model interest rate risk using a multi-factor HJM term structure model. Both use the Cholesky decomposition method to capture 72 correlated random variables used in the Monte Carlo simulation. Defaults are not restricted to maturity in either model and are allowed to occur at any simulation time t based upon the model's default trigger.[14]

I now describe the two different mechanisms for default. I first present the default mechanism for the structural model and then I present the default mechanism for the reduced form. These two distinct processes for default yield distinct alternative versions of the random cashflows, $\mathrm{T}_{\ddot{j},\ddot{k}}(t)$, in the empirical process that reflects loan level risks of default required for CMBS valuation. For both models I utilize the identical loss severity and disposition timing assumptions. The static loss severities were assumed from various studies[15] and vary by property type; they are: Multifamily (36%); Retail (47%); Office (37%); Hotel (48%); and Industrial (38%); and Other (50%). I assume 3 months to disposition of properties affecting all loans that transition to default consistent with The Bank for International Settlements (2008) and Peaslee and Nirenberg (2001).

Default in this study is very restrictive. It is defined as the transition to Real Estate Owned/Foreclosure. This is more restrictive than other studies that classify default as 60–90+ days delinquent. Missing instances in the data of a loan transitioning from current to a default state are not contemplated in either model. These instances would include (a) uninsured destruction of a property where there was no insurance against such disaster to make the lender whole resulting in instantaneous default; and (b) reporting errors at the special servicer level that could be attributed to clerical errors or fraud at either or both of the primary servicer and/or special service level to report delinquency and to transfer responsibility for servicing to the special servicer as provided for in the Pooling and Servicing Agreement. This transfer of debt collection to the special servicer is standard for all CMBS transactions and governs the credit monitoring oversight of all loans within CMBS transactions. In this sense, with the exception of (a) any loans that transition in payment status from current to default would be considered misclassified either due to human error or fraud. Neither model contemplates (a) or (b), though in principle one could add an additional random process to capture such risk in either model.

3.4.1 Default with the structural model

In the structural approach to modelling default risk, the diffusions of latent property values defined in Equation (13) are mapped to the loan level objects below. I begin with the simulated REIT value $\bar{V}_{j,t}$, where $\bar{V}_{j,0}$ is the initial value of the REIT index at the date of initialization of the simulation where the value is determined in the calibration Step 1. The equation:

$$\tilde{V}^i_{t,k} = \frac{1}{LTV^i_{0,k}} \times \frac{\bar{V}_{j,t}}{\bar{V}_{j,0}} \times e^{-0.5\sigma_j^2 t + \sigma_j \sqrt{t} dZ_i} \tag{15}$$

where $\frac{1}{LTV^i_{0,k}}$ represents the historical (at origination) inverse of the loan to value ratio for the i-th loan in the k-th CMBX Series. The inverse LTV corresponds to a specific property and the assumption is that the value of that property from origination time $t = 0$ evolves based upon the interaction with $\frac{\bar{V}_{j,t}}{\bar{V}_{j,0}}$ which represents the cumulative return of the corresponding REIT property type for which latent values are determined in the calibration for each simulation date. The i independent Brownian idiosyncratic shocks, dZ_i, are associated with the individual loan risks. Importantly, the volatility σ_j and the latent property value $\bar{V}_{j,t}$ are determined from the calibration step at the initialization of each simulation date. The value $\tilde{V}^i_{t,k}$ then represents the i-th simulated property value[16] that serves as collateral for the i-th CRELs that, in turn, serves as collateral for a CMBS transaction in my sample.

The risk event for CRELs contemplated by this model is default (and associated losses) that may occur at any simulation time $t \leq T$ expressed in Equation (15). If at any time t, $\tilde{V}^i_{t,k} < 1$ the loan defaults and the recovery process occurs with 3 months to disposition at a fixed loss severity rate varying by property type as previously discussed. Payments under default cease to be made. If $\tilde{V}^i_{t,k} \geq 1$ the loan pays according to its promised cashflow schedule. The rationale is that if the debt obligation is greater than the property value the borrower no longer has an incentive to make payments on the debt.

3.4.2 Default with the reduced-form model

In the reduced-form approach to modelling default risk, the default trigger capturing credit risk takes the form of default intensities. These intensities are used in the simulation in the Cox process as described in Lando (1998) to form the threshold for default in the simulation. The statistically determined transition intensities[17] articulate payment state transitions of current to delinquent (CD), delinquent to current (DC), and delinquent to default (DF), so $g \in \{(C \to D), (D \to C), (D \to F)\}$. Conceptually, the state transitions contemplated in the reduced-form approach are described in Figure 6. As is shown, default may only occur from a delinquent state (not a current state) and a transition to default is an absorbing state. This contrasts with the coarser approach taken in the structural

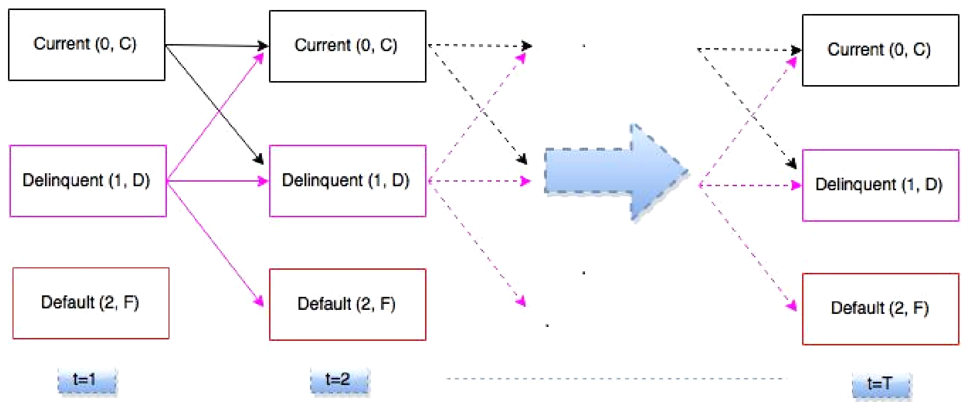

This figure depicts the state transition process in the reduced form model.

Figure 6 Loan state transition profile (reduced form).

model which only contemplates two states: current and default and uses only the simulated latent property value and corresponding inverse LTV to determine the simulated credit state of the loan.

The intensity estimates are determined from a multinomial logistic regression for hazard rate transitions utilizing 1,921,007 historical loan life transition observations from the Intex database of all loans underlying CMBX 1–8 between November 2007 and June 2015. Default is thus modelled as an intensity process. Each commercial loan i has a current, delinquent, and default intensity process that depends upon its payment status N_t, the state variable vector X_t, a vector of loan-specific characteristics U^i that are deterministic (non-random), e.g. the net operating income of the underlying property at the loan origination, and time-dependent loan characteristics L_t^i, e.g. the age of the loan. The current, delinquent, and default intensity processes for each loan have the same functional form, differing only in the loan specific variables used. Default may only be arrived at from a state of delinquency, over the discrete time interval $[t, t+\Delta]$ and I then define the default intensity as

$$\lambda_f(t, U^i, X_t, L_t^i, N_t)\Delta = 1/(1+e^{-(\varphi_f+\varphi_f U^i+\psi_f X_t+\xi_f L_t^i)}), \quad (16)$$

where $\varphi_c, \varphi_c, \psi_c, \xi_c, \varphi_d, \varphi_d, \psi_d, \xi_d, \varphi_f, \varphi_f, \psi_f, \xi_f$ are vectors of constants[18] determined statistically using maximum likelihood estimation and $\lambda_f(t, U^i, X_t, L_t^i, N_t)\Delta$ is the probability of jumping to default from delinquent. Estimation of these intensities is under the statistical measure and given the assumption that delinquency and default risk are conditionally diversifiable, as discussed in Jarrow *et al.* (2005), these intensity functions will be equivalent under both the empirical and martingale measures. I estimate these intensities using the multinomial logistic regression

$$F_g(v) = \frac{1}{\left(1+e^{-(\beta_0+\sum_{i=1}^{m}\beta_i v_i)}\right)} \quad (17)$$

where $F_g(v)$ represents the probability of a transition event for each of the three transition categories $g \in \{(C \to D), (D \to C), (D \to F)\}$, β is a constant vector, and v is the vector of independent variables which act as statistically determined lower boundaries, which if pierced with random draws generate a default (or other state transition). In this way, the Cox Process is used to incorporate both historical and current information in a statistical manner to govern state transitions for loans under Monte Carlo simulation. This approach, informed by the intensities used in the simulation can be compared with the default mechanism associated with the structural model in Equation (15). As in the structural model, the reduced-form default may occur at any simulation time $t \leq T$ subject to the condition that the CREL is in a delinquent state, D, at the previous time within the simulation, $t - 1$. The ensuing recovery process will occur with 3 months to disposition of the property at a fixed loss severity rate varying by property type as previously discussed. Payments under default cease to be made. In all other cases, the loan pays according to its promised cashflow schedule.

4 Loan and bond cashflows

In this section I describe the cashflow allocation algorithm which allocates loan level cashflows to a senior subordinate bond level structures with subordination levels that correspond to the vintages observed.[19]

4.1 *Loan level accuracy*

One of the staples of commercial mortgage lending is the balloon mortgage. Although some CRELs are fully-amortizing level-pay, the vast majority of loans are balloons. In a balloon mortgage payments prior to maturity, T, are based upon a level payment amortization schedule where such payments may include principal and interest, or at times, only interest. At maturity the remaining balance of the loan reflecting principal payments prior to maturity is made. As such, the balloon payment at maturity dwarfs all the prior payments. Additionally, balloon maturity may take place at 5, 7, 10, and 15 years and may have different covenants as to interest-only (IO) periods. Consider Figure 7 which shows the trust level aggregation of the promised principal cashflows associated with 4,004 loans underlying CMBX 1. The figure shows that the amounts and timing of the promised loan principal payments differ considerably over the life of the transaction reflecting different balloon and non-balloon maturities and differences between amortization schedules.

4.2 *Bond level structuring*

To allocate the accurate loan level cashflows to the bond level, I make the assumption as previously noted of a direct relationship between loan

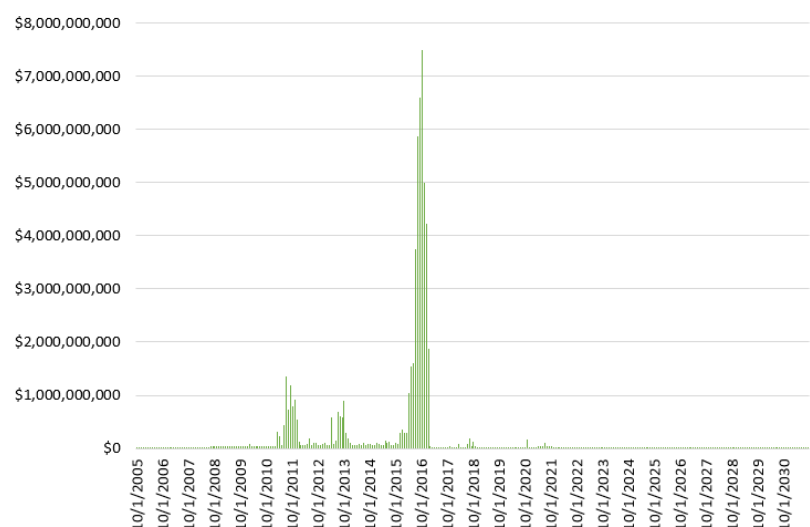

This chart shows the promised principal payments for the 4004 mortgages underlying CMBX Series 1.

Figure 7 Promised principal payments for 4,004 mortgages underlying CMBX Series 1.

cashflows and CMBX cashflows instead of an indirect relationship of loans allocated to CMBS tranches which are then allocated to CMBX tranches.

Let the Trust Principal of the j-th CMBX Series be defined for N-loans as $A_{\ddot{j}}(t) = \sum_{i=1}^{N} a_{\ddot{j},i}(t)$ with $a_{\ddot{j},i}(t)$ representing the i-th loan's promised principal payment due at time t for the $\ddot{j}$-th CMBX Series. The corresponding Trust Interest is defined for N-loans as $C_{\ddot{j}}(t) = \sum_{i=1}^{N} c_{\ddot{j},i}(t)$ with $c_{\ddot{j},i}(t)$ representing the i-th loan's promised interest payment due at time t for the $\ddot{j}$-th CMBX Series. At the end of each monthly payment period there is an outstanding principal balance for each of the loans, trust, and bonds reflecting monthly payments. The allocation of principal at the beginning of each monthly payment period, t, is made from $A_{\ddot{j}}(t)$ and such payments are said to be sequential pay, senior/subordinate with 'top-down' priority payment of principal for K total rated classes are paid first to AAA class, then to AJ/AS class, then to the AA class, ..., and then to the Unrated class until each of the $\ddot{k}$-th bond's outstanding principal balance is reduced to zero.

In each monthly payment period, t, the beginning balance of the bond, trust, and loan objects are adjusted for the principal payment made in the prior period, $t-1$. Let $\mathrm{O}_{\ddot{j},\ddot{k}}(t)$ represent the outstanding principal balance at the end of the payment period and $\hat{A}_{\ddot{j},\ddot{k}}(t)$ represent the promised principal payment to the $\ddot{k}$-th bond at the beginning of the payment period so $\mathrm{O}_{\ddot{j},\ddot{k}}(t) = \mathrm{O}_{\ddot{j},\ddot{k}}(t-1) - \hat{A}_{\ddot{j},\ddot{k}}(t)$ with

$$\hat{A}_{\ddot{j},\ddot{k}}(t) = \begin{cases} \max(0, \min(\mathrm{O}_{\ddot{j},1}(t-1), A_{\ddot{j}}(t)), & \text{for } \ddot{k}=1; \\ \max\left(0, \min\left(\mathrm{O}_{\ddot{j},\ddot{k}}(t-1), A_{j}(t) - \sum_{\ddot{k}=1}^{K} \hat{A}_{\ddot{j},\ddot{k}-1}(t)\right), \right. & \ddot{k} > 1 \end{cases} \tag{18}$$

representing the promised principal payments to the $\ddot{k}$-th bond at the beginning of the payment period for all $\ddot{k}$-tranches. Any excess principal remaining is then allocated to the next most senior tranche in the capital structure.

Similarly, for the interest paid to each of the $\ddot{k}$ bond classes is paid from the trust interest collected from the loans, $C_{\ddot{j}}(t)$, as defined above. The expression for the promised interest payment $\hat{I}_{\ddot{j},\ddot{k}}(t)$ with bond coupons, $i_{\ddot{j},\ddot{k}}$ is:

$$\hat{I}_{\ddot{j},\ddot{k}}(t) = \begin{cases} \max\left(0, \min(\mathrm{O}_{\ddot{j},1}(t-1)\frac{i_{\ddot{j},\ddot{k}}}{12}, C_{\ddot{j}}(t)\right), & \text{for } \ddot{k}=1; \\ \max\left(0, \min(\mathrm{O}_{\ddot{j},\ddot{k}}(t-1)\frac{i_{\ddot{j},\ddot{k}}}{12}, C_{\ddot{j}}(t) - \sum_{\ddot{k}=1}^{K} \hat{I}_{\ddot{j},\ddot{k}-1}(t)\right), & \ddot{k} > 1 \end{cases} \tag{19}$$

with total promised payment for the $\ddot{k}$-th bond in the $\ddot{j}$-th series in month t as:

$$\hat{T}_{\ddot{j},\ddot{k}}(t) = \hat{A}_{\ddot{j},\ddot{k}}(t) + \hat{I}_{\ddot{j},\ddot{k}}(t) \tag{20}$$

Figure 8 shows the cashflow allocation of the monthly promised loan level principal cashflows for the 4,004 loans underlying CMBX 1 to the bond tranches, where in each month the composition of the principal allocation is provided. Figure 8, Panel A shows the entire time series from October 2005 thru October 2031. The principal payment for the first 10.5 years are allocated exclusively to the AAA bondholders. Figure 8, Panel B shows a detail for the 12 months beginning June 2016 to May 2017. During this period, for this bond structure, the AAA class is paid off in October 2016 when payments to the AS class begin. The AS class is paid off in the next month at which time the AA class begins payment. This sequential pay senior subordinate capital structure pays this way until January 2017 at which time the remaining unrated classes (for which we do not have pricing) begin to receive payments until

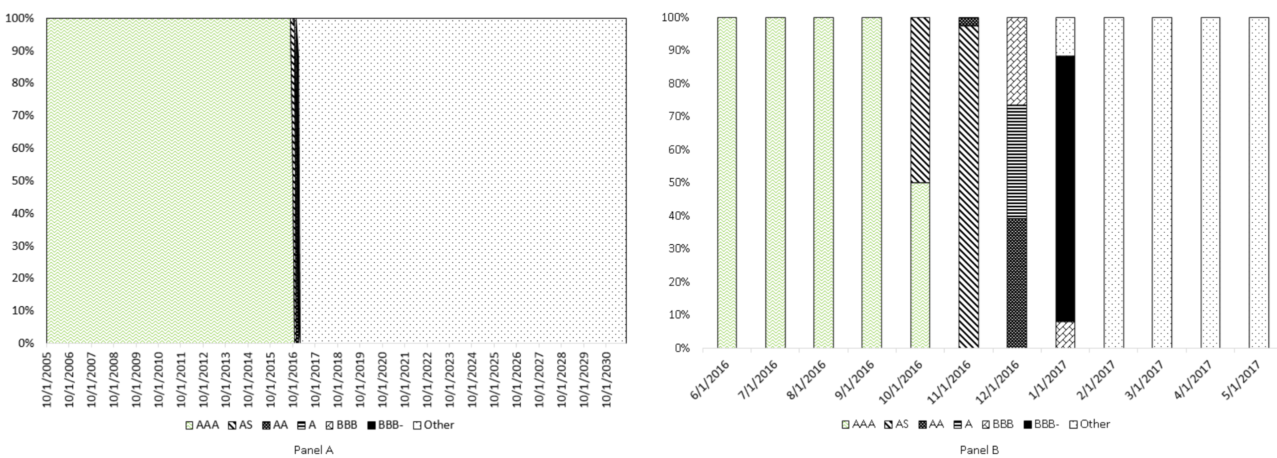

(a) This chart shows the proportion of the monthly promised principal payments (previously shown) allocated through the capital structure for CMBX Series 1 for all months. (b) This chart shows a detail of 12 months from 6/2016 to 5/2017 of the proportion of the monthly promised principal payments (previously shown) allocated through the capital structure for CMBX Series 1.

Figure 8 (a) Promised principal allocation for CMBX Series 1 (all months). (b) Detail of 12 months of promised principal allocation for CMBX1.

October 2031 as shown in the first panel under the promised cashflows schedules of the loans.

The care taken in this study to accurately capture the loan level cashflows and their timing combined with the homogeneity of subordination levels within ratings cohorts for specific vintages as seen in Frerich and van Heerden (2015) necessarily combine to yield CMBX cashflow profiles that should be quite close to the CUSIP level trading quality professional cashflows underlying CMBX tranches. Additionally, this approach expands upon a similar assumption in Driessen and Van Hemert (2012) who also assume a 1:1 relationship between loans and CMBX in their study although they do not accurately model the loan level cashflows. As such, the approach taken in this study is reasonable.

5 CMBS valuation

This section constructs the CMBS valuation model. This model is not the most complex formulation possible and it is applied to both the structural and reduced-form approaches. The amounts and timing of the promised cashflows evidently impact the timing of the promised bond level cashflows as described above. This shall be even more important when uncertainty is introduced into valuation and ultimately into risk/trade navigation.

I determine fair prices for the CMBX tranches (not underlying reference CMBS transaction tranches) under the assumption that the loan collateral securing the CMBS tranches serves as the cashflow generating collateral for the CMBX tranches. As discussed previously, the simplification is that I view the collateral pool as the loans themselves, and not the CMBS bond tranches.

CMBS face market (interest rate), credit, prepayment, and liquidity risks. In the initial formulation, I abstract from prepayment and liquidity risk. Liquidity risk and prepayment risks are excluded as I seek to focus on 'credit-only' in light of the significant default realizations during the financial crisis. This is common in the literature and in the case of CMBS it is reasonable. CRELs underlying CMBS have prepayment penalties that impose economic penalties on borrowers who seek to repay their mortgage obligations at some point earlier than maturity. Over time prepayment penalties have become increasingly more restrictive and varied, not less, with the introduction of defeasance. Among the prepayment restrictions facing commercial mortgage borrowers now are: hard lockout, standard fixed penalties, yield maintenance penalties, and defeasance penalties[20] with the majority of loan borrowers facing a *composite schedule* of prepayment restrictions over the life of the mortgage. For example, loan 87 (out of 25,019 total loans) found in the CMBS transaction BACM0504, which is one of the 25 CMBS transactions underlying CMBX Series 1, was originated on July 1, 2005 in the amount of \$5.92 mm and had a 10-year (120-month) scheduled balloon maturity date. The note agreement for loan 87 included a prepayment restriction schedule, Υ_{loan87}, at origination which provided the following composition of differing restrictions for each of the months associated with the life of the loan summarized as follows:

$$\Upsilon_{\text{loan87}} = \begin{cases} \text{no prepayment/hard lockout,} & \text{months } 1-26 \\ \text{defeasance,} & \text{months } 27-47 \\ \text{yield maintenance,} & \text{months } 48-116 \\ \text{no penalty/free prepayment} & \text{months } 116-120 \end{cases} \tag{21}$$

These restrictions on borrower behavior vary considerably across loans[21] and tenors and within the life of the loans.

The evidence observed empirically supports the perspective that these restrictions have acted as effective disincentives for refinancing activity in commercial real estate mortgages over the sample period. For example, in the sample of 25,019 loans categorically *all* loans had some form of prepayment restriction; all loans carried some hard lockout period. Further, 19,784 loans had some sort of defeasance period within the prepayment restriction schedule; 4,894 loans did not have any defeasance periods but did have either or both of yield maintenance, and 423 loans had no yield maintenance and no defeasance periods. Of these loans only approximately 1% of the sample loan balance (representing 201 loans) prepaid for any reason with approximately another 1% of the sample loan balance (representing 181 loans) prepaying during either free prepayment periods or cum-defeasance penalties. Less than 1% of the loan balance (representing 20 loans) prepaid with fixed penalties or yield maintenance.[22] Therefore, consistent with regulatory requirements in light of the significant default realizations during the financial crisis[23] and in light of the fact that the market/ratings community does not actively consider prepayment risk as being significant in the risk evaluation or market pricing of these securities, and further, in keeping with earlier well-regarded studies[24] that do not contemplate competing risks of prepayment,[25] prepayment is reasonably omitted from this study for ease of comparison with credit-only models in the literature.

We are given a filtered probability space $(\Omega, \mathcal{F}, (\mathcal{F}_t)_{t\in[0,\mathcal{T})}, \mathrm{P})$ satisfying the usual conditions (see Protter, 1990) with P the statistical probability measure. The trading interval is $[0, \mathcal{T}]$. Traded are default free bonds of all maturities $T \in [0, \mathcal{T}]$ with time t prices denoted $p(t, T)$, and various property indices, REITs, CRELs, CMBS bonds, and CMBX indices introduced below. The default-free spot rate of interest at time t is denoted r_t. I assume that markets are complete and arbitrage free so that there exists a unique equivalent martingale probability measure Q under which discounted prices are martingales.

The discount factor at time t is $e^{-\int_0^t r_s ds}$. Because I am interested in valuing CMBS, most of the model formulation will be under the probability measure Q.

The market price $m_{\ddot{j},\ddot{k}}(t)$ for the $\ddot{k}$-th bond in the $\ddot{j}$-th CMBX Series depends on the principal and interest cashflows from the N loans that are allocated to the $\ddot{k}$-th bond from the Trust cashflows, $\hat{\mathrm{T}}_{\ddot{j},\ddot{k}}(t) = \sum_{i=1}^{N}[\hat{\mathrm{A}}_{\ddot{j},\ddot{k}}(t) + \hat{I}_{\ddot{j},\ddot{k}}(t)]$, where $\hat{A}_{\ddot{j},\ddot{k}}(t)$ are the *promised* principal payments and $\hat{I}_{\ddot{j},\ddot{k}}(t)$ are the *promised* interest payments.

In contrast, the CMBS bonds then valued in the standard fashion using the corollary *actual* cashflows for N loans that are allocated to the k-th bond from the Trust cashflows,$\mathrm{T}_{\ddot{j},\ddot{k}}(t) = \sum_{i=1}^{N}[\mathrm{A}_{\ddot{j},\ddot{k}}(t) + I_{\ddot{j},\ddot{k}}(t)]$, where $\mathrm{A}_{\ddot{j},\ddot{k}}(t)$ are the actual principal payments and $I_{\ddot{j},\ddot{k}}(t)$ are the actual interest payments. Letting the random cashflows that contemplate loan level risks of default, loss, and interest rate risks, at time t to bonds $\ddot{k} = 1, \ldots, K$ be denoted $v_{\ddot{k}}(t)$, the time t value of these bonds is given by the following expression

$$b_{\ddot{k}}(t) = \mathrm{E}_t\left[\sum_{j=t+1}^{T_k} v_{\ddot{k}}(j)e^{-\int_t^j r_s ds}\right] \quad \text{if } t < T_k. \tag{22}$$

In the empirical process the fair value price of a bond at date s as a percent of par for the k-th bond in the j-th CMBX Series is defined as

$$b_{\ddot{j},\ddot{k}}(s) = \frac{\mathrm{E}_s\left[\sum_{t=s}^{T}\mathrm{T}_{\ddot{j},\ddot{k}}(t)e^{-r_t t}\right]}{\hat{F}_{\ddot{j},\ddot{k}}(s)} \tag{23}$$

where $\hat{F}_{\ddot{j},\ddot{k}}(s) = \sum_{t=1}^{T}\hat{A}_{\ddot{j},\ddot{k}}(t)$ is the face value of the bond and $\hat{A}_{\ddot{j},\ddot{k}}(t)$ promised principal.

6 Statistical validation and trade strategy

This section provides the statistical validation for the default probabilities determined in both models and provides the mispricing measure Theta. As mentioned previously, the data sets and filtrations for this analysis for both models are identical. This gives the unique opportunity to make direct comparisons of validation across both models which is rare in the literature.

6.1 *Statistical validation*

In the credit ratings literature two well established methods for validating the predictive ability of model default probabilities are (i) the Receiver Operating Characteristic Area Under the Curve (ROC AUC) and (ii) the Brier score. Briefly, an ROC AUC value of 0.50 for the ROC AUC indicates a random model with no predictive ability, while a value of 1.00 indicates perfect forecasting. In the case of the Brier score, $\widehat{B}$, which is the average mean square error of a predictor with a binary event[26] it holds that lower Brier scores indicate better predictive power[27] with a perfect forecast having a Brier score equal to zero. Figure 9 provides a summary of the ROC AUC, Brier score as well as the standard errors significance tests for the average lifetime probabilities of default corresponding to 25,019 loans in my sample.

In Figure 9, Panel A we observe the Brier score summary statistics. In the first row I report the Brier statistics for the structural model and in the second row I report the statistics for the reduced-form. In the first row, we see that the structural model yields a Brier score of 0.0983. Its skill score which represents 1 minus the ratio of the Brier score to its reference benchmark is 0.7061.[28] In row two I report the Brier statistics for the reduced form. The reduced-form approach yields a Brier score of 0.0516 and a skill score of 0.8460. Brier score testing indicates that the reduced form is

Panel A: Brier Table			
Model	Brier Score	Skill Score	n
Structural Model	0.0983	0.7061	25019
Reduced Form Model	0.0516	0.846	25019

Panel B: ROC AUC Table						
Model	ROC AUC	ROC p-value	95% Conf Interval		SE	n
Structural Model	0.7161	0.0000	0.6957	0.7366	0.0104	25019
Reduced Form Model	0.7592	0.0000	0.7362	0.7823	0.0118	25019

This table provides summary statistics from the Brier Score and ROC AUC analyses.

Figure 9 Summary of Brier and ROC AUC statistics.

more accurate in assessing default risk than the structural generalization.

In Figure 9, Panel B we observe the ROC AUC summary statistics. In the first row I report the ROC AUC statistics for the structural model and in the second row I report the statistics for the reduced form. In the first row we see that the ROC AUC for the structural model is 0.7161 and is highly significant at the 99% confidence level. The 95% confidence interval show lower and upper values of 0.6957 and 0.7366 with a standard error of 0.0104. In row two I report the ROC AUC statistics for the reduced-form. In the second row we see that the ROC AUC for the reduced form is 0.7592 and is highly significant at the 99% level. The 95% confidence interval show lower and upper values of 0.7362 and 0.7823 with a standard error of 0.0118. These findings are consistent with Bauer and Agarwal (2008) who also find better predictive power for hazard rate models. Additionally, the ROC AUC and Brier scores for both the reduced-form and the structural model in this study for CRELs are consistent with those reported in the credit ratings literature for corporate debt. As documented in Guttler's (2008) study based on 4-year default frequencies for corporate debt, the ROC AUC is 0.830 for Moody's and 0.820 for S&P. Similarly, reported Brier scores in the same study of 0.066 for Moody's and 0.069 for S&P are both in-line with the CMBS results. Finally, the corresponding ROC AUC for CMBS as reported by Christopoulos *et al.* (2008), pre-crisis, was 0.83. With slightly more than 7.5 years of observation and 1,013 defaults the statistical analysis conducted in this study is in sample. For the calibration and simulation of the economy this is not problematic as it is backward looking. Additional data to test out-of-sample would be ideal but has not provided at this time. With these caveats, these results appear to reasonably validate the predictive ability of both models in-sample and indicate better predictive power for the reduced-form probabilities of default compared with those determined in the structural generalization.

6.2 *Trade strategy–Mispricing measure Theta*

The fair value at simulation date described in Equation (23) reflects the expectation of the perturbed cashflows evaluated using Monte Carlo simulation. To identify mispricing, for each bond I compute for each simulation date s, the promised cashflow weighted average lives, $wal_{\ddot{j},\ddot{k}}(s)$, and the option adjusted weighted average lives, $oawal_{\ddot{j},\ddot{k}}(s)$, reflecting simulated default, where

$$wal_{\ddot{j},\ddot{k}}(s) = \begin{cases} \frac{\sum_{t=s}^{T} t\hat{A}_{\ddot{j},\ddot{k}}(t)}{\sum_{t=s}^{T} \hat{A}_{\ddot{j},\ddot{k}}(t)}, & for \sum_{t=1}^{T} \hat{A}_{\ddot{j},\ddot{k}}(t) > 0, \;\; and \\ 0, & otherwise \end{cases} \tag{24}$$

is the weighted average time to the receipt of the promised principal cashflows $\hat{A}_{j,k}(t)$ known as the weighted average life of the k-th bond/rating cohort in the j-th CMBX Series, and

$$oawal_{\ddot{j},\ddot{k}}(s) = \begin{cases} \dfrac{\mathrm{E}_s\left[\sum_{t=s}^{T} t\mathrm{A}_{\ddot{j},\ddot{k}}(t)\right]}{\mathrm{E}_s\left[\sum_{t=s}^{T} \mathrm{A}_{\ddot{j},\ddot{k}}(t)\right]}, & \mathit{for}\ \sum_{t=1}^{T} \mathrm{A}_{\ddot{j},\ddot{k}}(t) > 0, \\ & \mathit{and} \\ 0, & \mathit{otherwise} \end{cases} \tag{25}$$

is the corresponding bond's option adjusted weighted average life where $\mathrm{A}_{\ddot{j},\ddot{k}}(t)$ are the actual principal payments, including default.

I seek to control for risk by using these two characteristics and define

$$\mathrm{W}_{\ddot{j},\ddot{k}}(s) = \begin{cases} \left(\dfrac{wal_{\ddot{j},\ddot{k}}(s)}{oawal_{\ddot{j},\ddot{k}}(s)}\right), & \mathit{for}\ oawal_{\ddot{j},\ddot{k}}(s) > 0, \\ & \mathit{and} \\ 0, & \mathit{otherwise} \end{cases} \tag{26}$$

as a risk control for the k-th bond/rating cohort in the j-th CMBX Series. The "risk-adjusted" mispricing measure[29] is then computed as:

$$\theta_{\ddot{j},\ddot{k}}(s) \equiv b_{\ddot{j},\ddot{k}}(s) \times \mathrm{W}_{\ddot{j},\ddot{k}}(s) - m_{\ddot{j},\ddot{k}}(s). \tag{27}$$

The observed market prices of CMBS are meant to reflect all underlying risks. Figure 10, for example, shows the pricing for all AAA CMBX classes. In an efficient market, if the CREL risks of default and loss are well considered then those risks should be accurately priced at the CMBS level such that extraordinary profits cannot be systematically earned. With Theta, $\theta_{\ddot{j},\ddot{k}}(s)$ I seek to test the validity of the CMBS market's pricing of CREL default and loss risk using the default trigger mechanism of inverse LTV, Equation (15), in the Trading Strategy. Theta is the *signal* for the long/short trading opportunity and non-zero difference are precisely the signals that allow for the testing of CMBS market efficiency in the Trading Strategy. The market prices for CMBX $m_{\ddot{j},\ddot{k}}(s)$ are from Markit. As the trading intervals used for testing are 21 trading days to mitigate biases associated with month-end marks, bid-ask spreads and transactions costs are reasonably assumed to dissipate over the interval as discussed

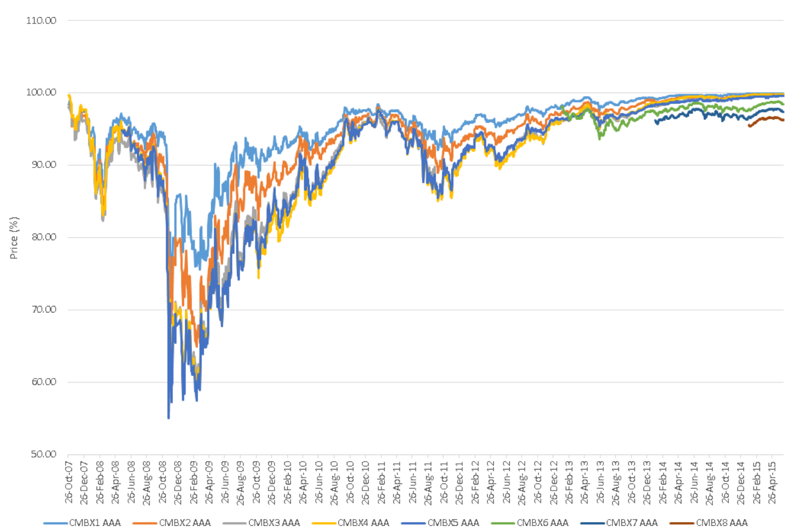

This chart shows the end of day daily mark to market pricing for the AAA tranches of CMBX Series 1–8.

Figure 10 CMBX Series 1–8 AAA market pricies (10/2007-6/2015, daily).

in West (2012). The database is comparable to other fixed income databases used in empirical investigations of credit risk models (see Duffee, 1999).

6.3 *Trading strategy–rules*

To construct the trading strategy, I consider the entire period for which I have static and dynamic loan level characteristics[30] and bond pricing data, 11/2007 to 6/2015 and trade the entire credit curve. As I am not trading cash bonds and as CMBX is far more frequently traded than the underlying cash securities, I am able to take full advantage of a limited number of bonds that nevertheless are exposed to a rich underlying sample of potentially defaultable loans comprising 1/3 of the CMBS universe. In this way I navigate both underlying credit and the bond overlay structure under risk-neutral conditions. I execute one trading strategy conducted over 21 day trading intervals constructing long and short portfolio positions based on market mispricings using Theta. The portfolio of long and short positions have equal weightings with 50% weighting in the long and 50% in the short positions.[31] I select from the available CMBX the top two and bottom two bonds from the set based on Theta.

The most undervalued $\ddot{j}$ CMBX Series and $\ddot{k}$ rating cohort ("cheapest of the cheap"), i.e. $\max_{\ddot{j},\ddot{k}}(\theta_{\ddot{j},\ddot{k}}(s))$ indicates the bond to be selected for the long position. The most overvalued j CMBX series and k rating cohort ("richest of the rich"), i.e. $\min_{j,k}(\theta_{j,k}(s))$ indicates the bond to be selected for the short position. This identification procedure is executed by the purchase and sale of positions at the market price at date s. Long and short positions are valued at $m_{\ddot{j},\ddot{k}}(s)$ and held within the portfolio until the end of the trading horizon. At the end of the trading horizon, time $s+1$, the bonds are bought and sold at the market prices $m_{\ddot{j},\ddot{k}}(s+1)$. The process is repeated across the sample period on each simulation date s for both the structural and reduced-form models.

6.4 *Trading strategy–results*

As shown in Figure 11 the trading strategy generates positive returns for the structural model. Across the 91 trading intervals, the distribution of correctly identified mispricings in both the long and short buckets is clustered tightly about 50% over the 7.5 years testing period. The automated trading strategy posted a 17% cumulative return over the 91 trading intervals. The 91 monthly interval portfolio returns (black) and the cumulative return on the portfolio are summarized in Figure 12. The specific trades identified with Theta and summary information on prices and returns for the trading strategy are summarized in Figure 13a–f.

As shown in Christopoulos and Jarrow (2016) the exact same trading strategy with the exact same data set implemented used in this study for the structural model produced a cumulative return of 71% over the sample period for the reduced-form model. A summary of the specific trades identified with Theta and summary information on prices and returns for the trading strategy for the reduced form are summarized in Figure 14a–f.

While the trading profits with the structural model are positive, they are much worse relative to those generated under the reduced-form approach. Since the modelled economy, data set, trading strategy, valuation methods, and sample periods are the same for both models, the only distinction between the structural and reduced-form models lies in the default mechanism. This is interesting.

6.5 *Portfolio management implications*

From a portfolio management assessment perspective, one way to compare the profile of the two model approaches would be to assume returns

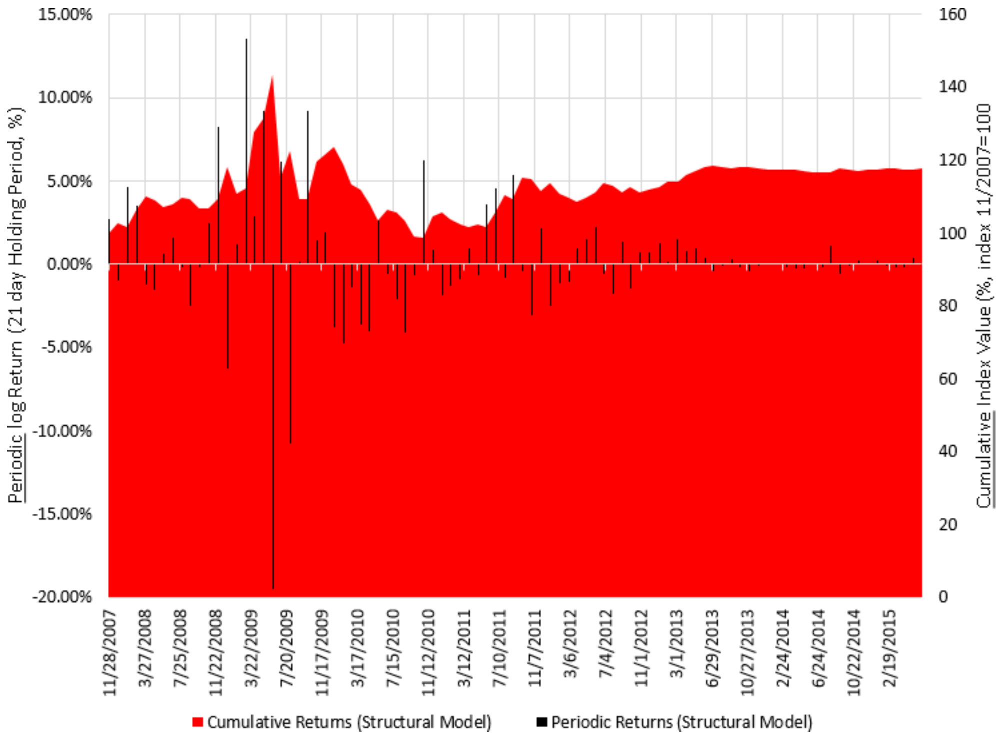

This chart shows the periodic and cumulative returns for the structural model for the automated trading strategies using Theta. The left Y-axis show the periodic returns corresponding to the black bars. The right Y-axis shows the cumulative portfolio value corresponding to the red area which begins with a cumulative starting value of 100 and ends with a cumulative value of 117.87.

Figure 11 Structural generalization trading strategy returns (11/2007–6/2015).

For each trade interval		For each sub portfolio and total portfolio					
# Correct	Frequency		rtrn_short1	rtrn_short2	rtrn_long1	rtrn_long2	rtrn_totport
0	2	Total Correct	46	44	46	49	46
1	10	Total Possible	91	91	91	91	91
2	67	Percentage Correct (%)	50.55%	48.35%	50.55%	53.85%	50.55%
3	7						
4	5						
Total	91						

This table summarizes the number of correctly identified trading returns for the trading intervals using the structural model. The first two columns show for example that in only 5 (of 91 total) cases did the structural model identify the 4 best trading opportunities for the trading interval. The columns to the right simply break down the correctly identified trades in rank order.

Figure 12 Distributions of correct calls in trading strategy (structural model).

generated by the models were Normally distributed as is commonly done. In Figure 15a, I plot the actual return distribution and in Figure 15b, I provide the normal cumulative distribution function (cdf) for both portfolios with $\mu = 0.71\%$, $\sigma = .051$ for the reduced form and $\mu = 0.26\%$, $\sigma = .038$ for my structural generalization. In Figure 15c what we see is that the

Date	Panel A (Theta Signa)				Panel B (Bonds Selected)				Panel C (Market Trade Prices, Initiated)				Panel D (Market Trade Prices, Unwind)				Panel E (Interval Returns)				Panel F (Portfolio)	
	short1	short2	long1	long2	short1	short2	long1	long2	pxshort1	pxshort2	pxlong1	pxlong2	pxshort1	pxshort2	pxlong1	pxlong2	short1	short2	long1	long2	Period	Cumulative
Oct-17	-98.26	-97.26	-43.12	-44.55	2_cmbx4AJ	3_cmbx4AA	1_cmbx1AAA	1_cmbx3AAA	98.26	97.26	98.40	98.11	-	-	-	-	-	-	-	-	0.00	100.00
Nov-17	-92.01	-91.16	-38.23	-40.12	4_cmbx4A	2_cmbx4AJ	1_cmbx3AAA	1_cmbx1AAA	92.01	91.16	94.79	96.02	91.16	88.52	96.02	94.79	-0.07	-0.09	-0.02	-0.03	0.03	102.76
Dec-17	-94.81	-94.57	-40.39	-44.44	2_cmbx4AJ	4_cmbx4A	1_cmbx3AAA	1_cmbx2AAA	94.81	94.57	96.15	96.90	94.57	94.81	96.15	97.44	0.03	0.04	0.01	0.01	-0.01	101.79
Jun-17	-80.85	-72.98	9.84	8.93	2_cmbx2AJ	3_cmbx1AA	1_cmbx1AAA	1_cmbx2AAA	80.85	72.98	96.00	94.73	71.81	72.98	96.00	94.73	-0.11	-0.08	0.00	-0.01	0.05	110.38
Jul-17	-80.66	-80.40	8.31	2.18	2_cmbx1AJ	2_cmbx2AJ	1_cmbx1AAA	1_cmbx2AAA	85.96	80.40	95.81	94.44	80.40	75.42	95.81	94.44	-0.01	0.03	0.00	0.00	-0.01	109.48
May-17	-100.91	-100.51	130.45	128.80	6_cmbx6BBB-	4_cmbx7A	2_cmbx6AJ	3_cmbx6AA	100.91	100.51	100.14	101.16	100.91	100.51	100.14	101.16	-0.01	0.00	0.00	0.00	0.00	117.76
Jun-17	-13.59	0.88	73.35	68.41	6_cmbx5BBB-	1_cmbx1AAA	4_cmbx5A	4_cmbx4A	13.59	99.95	30.67	33.92	100.61	99.69	99.76	100.79	0.00	-0.01	0.00	0.00	0.00	117.87

This table shows a subset of 6 of 91 selected trade intervals for the structural model. Panel A shows the value of the two smallest and two largest Theta values. Panel B shows the bonds for those Theta signals on that trading date. Panel C shows the prices at which trades for the short and long positions were executed and brought into the portfolio. Panel D shows the prices for bonds when they were taken out of the portfolio (unwound) at the end of the interval. Panel E shows the log returns for each of the short and long positions over the interval and the interval return for the portfolio comprised of the two short and two long components. Panel F shows the cumulative return on the portfolio initiated at a value equal to 100 in October 2007 and with a cumulative value equal to 117.87 in June 2015.

Figure 13 Summary of structural model returns generated by automated trading strategy using Theta.

Date	Panel A (Theta Signa)				Panel B (Bonds Selected)				Panel C (Market Trade Prices, Initiated)				Panel D (Market Trade Prices, Unwind)				Panel E (Interval Returns)				Panel F (Portfolio)	
	short1	short2	long1	long2	short1	short2	long1	long2	pxshort1	pxshort2	pxlong1	pxlong2	pxshort1	pxshort2	pxlong1	pxlong2	short1	short2	long1	long2	Period	Cumulative
Oct-17	-88.67	-85.92	20.22	17.81	4_cmbx1A	5_cmbx4BBB	1_cmbx2AAA	1_cmbx3AAA	91.98	85.92	98.01	98.11	-	-	-	-	-	-	-	-	0.00	100.00
Nov-17	-83.04	-79.20	28.52	26.03	4_cmbx1A	5_cmbx1BBB	2_cmbx4AJ	1_cmbx2AAA	88.39	79.20	91.16	95.22	88.39	76.91	95.22	94.79	-0.04	-0.11	-0.03	-0.03	0.02	102.18
Dec-17	-94.81	-94.57	192.28	182.75	2_cmbx4AJ	4_cmbx4A	1_cmbx4AAA	1_cmbx2AAA	94.81	94.57	97.71	96.90	91.69	83.24	94.81	96.90	0.04	0.05	0.04	0.02	-0.01	101.42
Jun-17	-23.08	-20.70	59.13	51.66	5_cmbx5BBB	6_cmbx1BBB-	3_cmbx4AA	2_cmbx4AJ	23.08	21.79	46.67	65.73	21.79	36.08	46.67	65.73	-0.29	-0.29	-0.22	-0.12	0.06	139.00
Jul-17	-24.29	-22.67	52.24	46.50	4_cmbx5A	5_cmbx5BBB	2_cmbx4AJ	2_cmbx3AJ	43.36	22.67	67.85	72.31	22.67	21.86	47.67	67.85	-0.02	0.00	0.02	0.03	0.02	141.35
May-17	-13.82	-1.92	88.50	76.32	6_cmbx5BBB-	5_cmbx5BBB	4_cmbx4A	4_cmbx3A	13.82	16.65	33.03	19.70	13.82	6.00	33.03	54.17	-0.04	0.15	-0.01	0.00	-0.03	165.55
Jun-17	-13.59	0.88	73.35	68.41	6_cmbx5BBB-	1_cmbx1AAA	4_cmbx5A	4_cmbx4A	13.59	99.95	30.67	33.92	13.59	17.33	33.92	22.33	-0.02	0.04	0.03	0.13	0.03	170.88

This table shows a subset of 6 of 91 selected trade intervals for the reduced form model. Panel A shows the value of the two smallest and two largest Theta values. Panel B shows the bonds for those Theta signals on that trading date. Panel C shows the prices at which trades for the short and long positions were executed and brought into the portfolio. Panel D shows the prices for bonds when they were taken out of the portfolio (unwound) at the end of the interval. Panel E shows the log returns for each of the short and long positions over the interval and the interval return for the portfolio comprised of the two short and two long components. Panel F shows the cumulative return on the portfolio initiated at a value equal to 100 in October 2007 and with a cumulative value equal to 170.88 in June 2015.

Figure 14 Summary of reduced form model returns generated by automated trading strategy using Theta.

returns realized by my structural generalization underperformed predictions implied by the cdf with a greater proportion of returns <0% than would be estimated by the Normal. In contrast, in Figure 15d we see a relative outperformance by the reduced-form with a lower proportion of returns <0% than would be estimated by the Normal and a slower steepening disclosing a greater ability to realize larger returns than my structural generalization. The greater precision in valuation exhibited by the reduced-form model compared with my structural generalization is not isolated to the crisis. In fact, when considering only the recovery, more than 40% of the cumulative returns of the reduced form come from that period contrasting with 10% for my structural

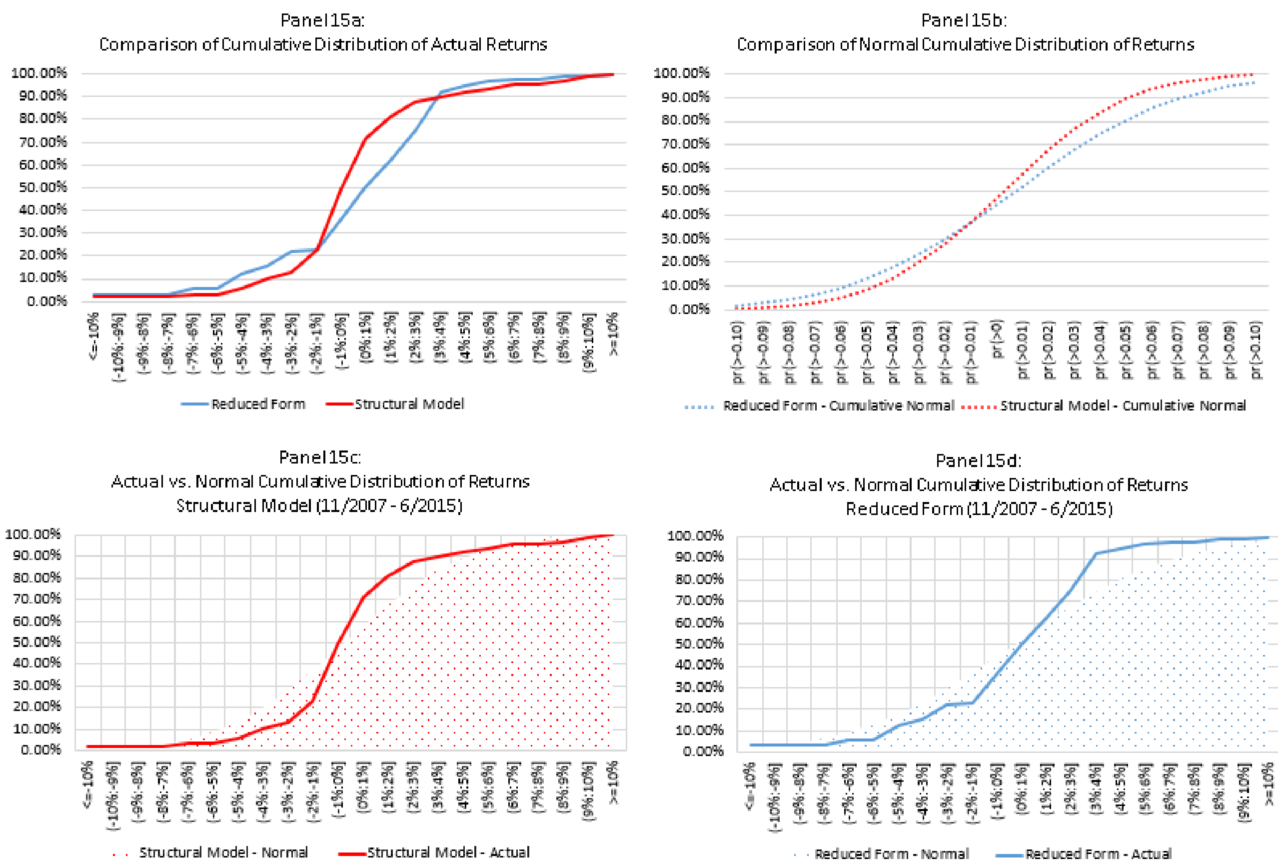

The panels in this figure show the actual and cumulative normal distributions of returns for each of the structural model and reduced form approches. Panel A compares Actual to Actual while Panel B compares Normal to Normal. Panels C and D combine the Actual and Normal views for the structural and reduced form models, respectively.

Figure 15 Summary of reduced form model returns generated by automated trading strategy using Theta.

generalization. So, while proportionally the models perform about the same in the recovery versus their total performance (40%/71% reduced form and 10%/17% for structural) the fact is that the returns captured by the reduced-form in both the crisis and the recovery are larger and the relative outperformance is not dominated by outsized gains in the crisis carrying forward to the recovery.

7 Conclusion

The results in this paper indicate that the reduced-form model exhibits better capabilities of estimating default risk of CRELs and estimating their pricing at the CMBX level than the structural model. I hold the simulated economy and data sets constant and observe that the corresponding approaches to the modelling of pathwise default events yield different results. In the automated trading strategy tests we observe 17% cumulative returns for the structural model compared with 71% cumulative returns for the reduced-form model. Additionally, in the physical default statistical validations of ROC AUC and Brier validations we also see stronger estimation capability in the reduced-form compared with the structural model. This comparison is innovative in the literature and useful in consideration of appropriate risk assessment of CMBS. The

Cox process and its role within the reduced form has the ability to distil historical and current information in a manner that is not possible in the structural generalization. Given the comparatively better results generated with the reduced form compared with the structural generalization, it appears that the design features of different models are central to evaluating CMBS risk and investment strategies.

Acknowledgements

I would like to acknowledge the anonymous donor of the outstanding data set that made this study possible as well as the interested and expert professional feedback provided to me throughout this project. I would also like to thank the University of Texas at Austin, McCombs School Department of Finance for being supportive of my research. G. Fong the Editor of the *Journal of Investment Management* and the anonymous referee also deserve special thanks for giving me great comments that helped to focus and streamline this paper. Additionally, I thank D. Jones, S.A. Ravid, A. Ruszczńyski for their guidance and support at earlier stages of this project at Rutgers University in my dissertation as well as each of A. Connelly, D. Ilut, and M. Zifchock for their consistent thoughtful comments and insights. Finally, I would like to acknowledge the continued and indefatigable support and feedback of J. Barratt, R. Jarrow, and my family who have helped me immeasurably.

Notes

1 Attributed to Merton (1974) and adopted for CMBS by Driessen and Van Hemert (2012).

2 First introduced by Jarrow and Turnbull (1992, 1995).

3 The market portfolio consists of all assets in the market where the weights of the assets are proportional to their size in the market. The empirical returns for the market portfolio used in this study were secured from the portfolio constructed by Ken French which includes all New York Stock Exchange (NYSE), American Stock Exchange (AMEX), and NASDAQ firms. The long-only CMBS portfolio is comprised of all CMBX classes weighted by class principal balance.

4 I use subordination levels provided by vintage as discussed in Stanton and Wallace (2012).

5 For further discussion on CMBX Derivatives please see Whetten and Manzi (2006), Driessen and Van Hemert (2012), among others.

6 These calibrated parameters are for REITs *not* the commercial real estate loans underlying the CMBS.

7 I index with both j and k for Equations (4 and 5).

8 I age the debt over the year and "roll" the debt every December 31 such that on January 1 the maturity of the debt is 5 years whereas by December 31 the maturity of the debt is 4 years.

9 See Driessen and Van Hemert (2012).

10 See www.federalreserve.gov/releases/h15.

11 As previously stated, I assume $q = 0\%$ but I include here for continuity with the literature.

12 See Christopoulos *et al.* (2008).

13 See Glasserman (2003). Care is taken to implement common technical adjustments in the code base are implemented to adjust numerical tolerances required for floating point values and to make extensions to Cholesky as necessary for variance–covariance matrices that are positive semi-definite (see: https://en.wikipedia.org/wiki/Cholesky_decomposition).

14 Christopoulos *et al.* (2008) show that many loans default prior to maturity. That finding corresponds with the sample for this paper in which ~85% of the 1,013 defaults occurred prior to maturity.

15 These compare well with Moody's loss severities of Multifamily (35%); Retail (49%); Office (40%); Hotel (46%); and Industrial (39%) as reported in Banhazl and Halpern (2015) and correspond to similar values reported by Frerich and van Heerden (2015).

16 The index notation for the entire correlated economy is $\iota = 1, \ldots, 72$. There are $j = 1, \ldots, 6$ property specific REIT indices and $j \in \iota$. The volatility σ_j is determined only for the j subset objects.

17 The transition intensity process for evaluation of credit risk corresponds with the regulatory requirements of the Federal Reserve under CCAR. See *Appendix B* of Board of Governors of the Federal Reserve System (2015).

18 These estimates are statistically related to loan payment state transitions and include both static loan level characteristics such as loan coupon and property location

and dynamic loan level characteristics such as payment status and age. See Christopoulos and Jarrow (2016).

19 The subordination levels are observed in Stanton and Wallace (2015), and Banhazl and Halpern (2012), among others.

20 Defeasance is generally considered to be the most restrictive prepayment penalties requiring replacement of loan cashflows with treasury strips. See Hallman (2014) and Christopoulos *et al.* (2008), among others.

21 Free prepayment periods are typically granted to borrowers within 12 months prior to maturity to allow borrowers time to negotiate and secure refinancing.

22 Note that in the example of loan 87 contained in CMBX 1 it neither prepaid nor defaulted over the observation period.

23 See *Appendix B* of Board of Governors of The Federal Reserve System (2015).

24 See Titman and Torous (1989) and Driessen and Van Hemert (2012), among others.

25 As presented in Ciochetti *et al.* (2002) and Christopoulos *et al.* (2008), among others.

26 Expressed as $\widehat{B} = \frac{1}{N}\sum_i^N(\hat{p}_i - Y_i)^2$, where $\hat{p}_i$ is the estimated probability of an event.

27 See Gruner *et al.* (2005), Krämer and Güttler (2008), Medema *et al.* (2009), and Bauer and Agarwal (2014).

28 Where Brier Skill Score (BSS) is defined as $BSS = 1 - \frac{\hat{B}}{\hat{B}_{\text{ref}}}$.

29 See Christopoulos and Jarrow (2016) for their innovation and testing of $W_{j,k}(s)$, Modigliani and Modigliani (1997) for discussion of risk ratio adjustments that inspired construction of $W_{j,k}(s)$, and Fabozzi (1992) for discussion of option adjusted weighted average life.

30 Static information would include things like loan coupon, location, property type. Dynamic includes the current payment status of the loan.

31 Where the 50% long is split evenly between two bonds (25% of the total portfolio each) and the 50% short is also split evenly between two bonds (25% of the total portfolio each).

References

Ambrose, B., Shafer, M., and Yildirim, Y. (September 2014). "The Impact of Diversification on Commercial Mortgage Spreads and Default Rates," Working Paper, Pennsylvania State University.

Arora, N., Bohn, J. R., and Zhu, F. (2005). "Reduced Form vs. Structural Models of Credit Risk: A Case Study of Three Models," *Journal of Investment Management* **17.3**(4), 43–53.

Banhazl, K. and Halpern, M. (2015). *US CMBS Loss Severities: Q1 2015 Update*, New York, NY: Moody's Investors Service.

Bank for International Settlements (2008). Basel Committee on Banking Supervision The Joint Forum Credit Risk Transfer Developments from 2005 to 2007.

Bao, J., O'Hara, M., and Zhou, X. A. (September 2016). "The Volcker Rule and Market-Making in Times of Stress," Working Paper, Cornell University.

Bauer, J. and Agarwal, V. (2014). "Are Hazard Models Superior to Traditional Bankruptcy Prediction Approaches? A Comprehensive Test," *Journal of Banking & Finance* **40**, 432–442.

Board of Governors of the Federal Reserve System (March 2015). Dodd-Frank Act Stress Test 2015: Supervisory Stress Test Methodology and results, pp. 51–52.

Buschbom, S., Kau, J., Keenan, D., and Lyubimov, K. (2015). "Delinquencies, Default and Borrowers' Strategic Behavior toward the Modification of Commercial Mortgages," Working Paper, University of Georgia.

Black, F. and Scholes, M. (1973). "The Pricing of Options and Corporate Liabilities," *The Journal of Political Economy*, 637–654.

Chandan, S. (2012). *The Past, Present and Future of CMBS*. Wharton Real Estate Review.

Chen, L., Lesmond, D. A. and Wei, J. (2007). "Corporate Yield Spreads and Bond Liquidity," *The Journal of Finance* **62**(1), 119–149.

Christopoulos, A. D. and Jarrow, R. A. (2016). "CMBS Market Efficiency: The Crisis and the Recovery," Working Paper, Cornell University.

Christopoulos, A. D. and Jarrow, R. A. *et al.* (2014). "Structured Finance Securities Options Pricing Architecture and Process," United States Patent and Trademark Office. US 8788404 B1.

Christopoulos, A. D., Jarrow, R. A., and Yildirim, Y. (2008). "CMBS and Market Efficiency with Respect to Costly Information," *Real Estate Economics* **36**(3), 441–498.

Driessen, J. (2005). "Is Default Event Risk Priced in Corporate Bonds?," *Review of Financial Studies* **18.1**, 165–195.

Driessen, J. and Van Hemert, O. (2012). "Pricing of Commercial Real Estate Securities during the 2007–2009 Financial Crisis," *Journal of Financial Economics* **105**, 37–61.

Duffee, G. (1999). "Estimating the Price of Default Risk," *The Review of Financial Studies* **12**, 197–226.

Fabozzi, F. (1993). *Fixed-Income Mathematics* (Revised Edition). Chicago, IL: Probus.

Fama, E. and Malkiel B. G. (1970). "Efficient Capital Markets: A Review of Theory and Empirical Work," *The Journal of Finance* **25**(2), 283–417.

Frerich, L. and van Heerden, C. (2015). *CMBS Performance Monitor – May Summary* Wells Fargo.

Fung, D. (2016). "Improving Communities' and Businesses' Access to Capital and Economic Development," Written testimony on behalf of the Commercial Real Estate Finance Council before United States Senate Committee on Banking, Housing, and Urban Affairs Subcommittee on Securities, Insurance, and Investment.

Ghent, A. and Valkanov, R. (2015). "Comparing Securitized and Balance Sheet Loans: Size Matters," *Management Science*.

Gilchrist, S. and Zakrajšek, E. (2012). "Credit Spreads and Business Cycle Fluctuations," *The American Economic Review* **102**(4), 1692–1720.

Glasserman, P. (2003). *Monte Carlo Methods in Financial Engineering* (Vol. 53). Springer Science & Business Media.

Guttler, A. (2005). "Using a Bootstrap Approach to Rate the Raters," *Financial Markets and Portfolio Management* **19**(3), 277–295.

Hallman, G. (2014). CMBS Prepayments. Lecture Notes. University of Texas at Austin.

Heath, D., Jarrow, R. A., and Morton, A. (1992). "Bond Pricing and the Term Structure of Interest Rates: A New Methodology for Contingent Claims Valuation," *Econometrica* **60**, 77–105.

Hollifield, B., Neklyudov, A., and Spatt, C. (2016). "Bid-Ask Spreads, Trading Networks and the Pricing of Securitizations: 144a vs. Registered Securitizations," Working paper, Carnegie-Mellon University.

Jarrow, R. A. (2001). "Default Parameter Estimation Using Market Prices," *Financial Analysts Journal* **57**(5), 75–92.

Jarrow, R. A. (2002). *Modeling Fixed Income Securities and Interest Rate Options* (2nd ed.). Palo Alto, CA: Stanford University Press.

Jarrow, R. A. (2013). "Option Pricing and Market Efficiency," *Journal of Portfolio Management* **40**(1), 88–94.

Jarrow, R. A., Lando, D., and Yu, F. (2005). "Default Risk and Diversification: Theory and Applications," *Mathematical Finance* **15**, 1–26.

Jarrow, R. A. and Protter, P. (2004). "Structural versus Reduced Form Models: A New Information Based Perspective," *Journal of Investment Management* **2**(2), 1–10.

Jarrow, R. A. and Turnbull, S. (1992). "Credit Risk: Drawing the Analogy," *Risk* **5**(9), 63–70.

Jarrow, R. A. and Turnbull, S. (1995). "Pricing Derivatives on Financial Securities Subject to Credit Risk," *The Journal of Finance* **50**, 53–85.

Kau, J., Keenan, D., and Yildirim, Y. (2009). "Estimating Default Probabilities Implicit in Commercial Mortgage Backed Securities (CMBS)," *Journal of Real Estate Economics* **39**, 107–117.

Krämer, W. and Güttler, A. (2008). "On Comparing the Accuracy of Default Predictions in the Rating Industry," *Empirical Economics* **34**(2), 343–356.

Lando, D. (1998). "On Cox Processes and Credit Risky Securities," *Review of Derivatives Research* **2**(2–3), 99–120.

Medema, L., Koning, R. H., and Lensink, R. (2009). "A Practical Approach to Validating a PD Model," *Journal of Banking & Finance* **33**(4), 701–708.

Merton, R. C. (1974). "On the Pricing of Corporate Debt: The Risk Structure of Interest Rates," *Journal of Finance* **29**(2), 449–470.

Modigliani, F. and Modigliani, L. (1997). "Risk-Adjusted Performance," *Journal of Portfolio Management* **23**(2), 24–29.

Peaslee, J. M. and Nirenberg, D. Z. (2001). *Federal Income Taxation of Securitization Transactions.* Frank J. Fabozzi Associates.

Penner, E. (2016). *CMBS in Flux*. LinkedIn.

Protter, P. (1990). *Stochastic Integration and Differential Equations: A New Approach*. New York: Springer-Verlag.

Riddiough, T. and Zhu, J. (2016). "Risk and Information Tranching, Security Governance, and Incentive Compatible Capital Structure Design," Working Paper, University of Wisconsin.

Stanton, R. and Wallace, N. (December 2012). "CMBS Subordination, Ratings Inflation, and Regulatory Capital Arbitrage," Fisher Center Working Paper Series.

Stanton, R. and Wallace, N. (2011). "The Bear's Lair: Index Credit Default Swaps and the Subprime Mortgage Crisis," *Review of Financial Studies* **24**(10), 3250–3280.

Tankov, P. and Voltchkova, E. (2009). *Jump-Diffusion Models*. Banque et Marché.

Titman, S. and Torous, W. (1989). "Valuing Commercial Mortgages: An Empirical Investigation of the Contingent Claims Approach to Pricing Risky Debt," *The Journal of Finance* **44**, 345–373.

Titman, S. and Tsyplakov, S. (2010). "Originator Performance, CMBS Structures, and the Risk of Commercial

Mortgages," *The Review of Financial Studies* **23**(9), 3558–3594.

Titman, S., Tompaidis, S., and Tsyplakov, S. (2005). "Determinants of Credit Spreads in Commercial Mortgages," *Real Estate Economics* **33**(4), 711–739.

Vassalou, M. and Xing, Y. (2004). "Default Risk in Equity Returns," *Journal of Finance* **59**, 831–868.

West, J. (2012). "Catastrophes and Insurance Stocks – A Benchmarking Approach for Measuring Efficiency," *Annals of Actuarial Science* **6**(01), 103–136.

Whetten, M. and Manzi, J. (2006). *The CMBX: The Future is Here*. Nomura Fixed Income Research.

Keywords: CMBS; structural model; reduced form, default risk, credit risk; portfolio management

JEL Code: G12, G13